DOI: 10.1002/ejoc.200701113

External vs. Internal Interactions in the Enantiodiscrimination of Fluorinated α-Amino Acid Derivatives by Heptakis[2,3-di-*O*-acetyl-6-*O*-(*tert*-butyldimethylsilyl)]-β-cyclodextrin, a Powerful Chiral Solvating Agent for NMR Spectroscopy

Gloria Uccello-Barretta,*[a] Federica Balzano,[a] Francesca Pertici,[a] Laszlo Jicsinszky,[b] Giuseppe Sicoli,[c] and Volker Schurig[d]

Keywords: Cyclodextrins / Enantiomeric purity / Enantiodiscrimination / NMR spectroscopy

NMR spectroscopic investigations involving extensive use of ROESY and DOSY techniques and comparison with silylated-acetylated linear dextrins as acyclic model compounds shed light on the origin of the phenomenon of enantiodiscrimination of fluorinated α-amino acid derivatives by heptakis[2,3-di-*O*-acetyl-6-*O*-(*tert*-butyldimethylsilyl)]-β-cyclodextrin. The effectiveness and versatility of the cyclic derivatized oligosaccharide as a chiral solvating agent for the NMR determination of enantiomeric purity in the same class of compounds is demonstrated. A regular correlation between the relative positions of enantiomers' signals and absolute configurations is observed.

Introduction

Cyclodextrins are truncated cone-shaped cyclic oligosaccharides, which have found widespread applications as chiral auxiliaries for the chromatographic separation of enantiomers[1–7] and for the NMR spectroscopic differentiation of enantiomers.[8–14]

NMR spectroscopic differentiation methods mainly involve the use of cyclodextrins as chiral solvating agents (CSAs),[8–14] potentially capable of inducing anisochrony of enantiotopic nuclei, which are rendered diastereotopic and hence distinguishable in the NMR spectra, the integrated areas of signals of the enantiomers reflecting their enantiomeric composition and their relative positions being correlatable with the absolute configuration. Originally, native cyclodextrins were proposed[15,16] as CSAs for use in water, due to their solubility characteristics. In this solvent, inclusion processes inside the cyclodextrin cavity constitute the basis of enantiodiscrimination. Selective or exhaustive derivatization of cyclodextrins at the primary and secondary hydroxy groups brought about significant changes in their physicochemical properties,[17] extending their use to analyses in organic solvents, even though in some cases the propensity of cyclodextrins to form inclusion complexes is lost.[18–20]

The potential of selective placing of different functional groups on the wide and narrow cyclodextrin rims was also exploited, and this approach led to CSAs with enhanced enantiodiscriminating properties.[20–22] Among derivatized cyclodextrins, heptakis[2,3-di-*O*-acetyl-6-*O*-(*tert*-butyldimethylsilyl)]-β-cyclodextrin (**1**, Scheme 1) has already become established as a powerful chiral stationary phase (CSP) for the gas-chromatographic separation[23] of stereoisomeric flavour compounds. The development of analogously modified linear dextrins ("acyclodextrins") for use in enantioselective gas chromatography (GC) provided additional insights regarding the role of cavity and the number of derivatized glucose units in the enantiodiscrimination processes.[24,25] The remarkable utility of **1** as a CSA for the NMR enantiodiscrimination of an apolar fluorinated compound [1,1,1,3,3-pentafluoro-2-(fluoromethoxy)-3-methoxypropane, named "compound B", a decomposition product of the inhalational anaesthetic sevoflurane] was also demonstrated,[21] suggesting its potential in the analyses of fluorinated compounds devoid of hydrogen-bond donor groups. Although interpretation of the origin of enantiodiscrimination by cyclodextrins represents a challenging goal, NMR spectroscopic investigations have clearly established the role of partial inclusion of "com-

[a] Università degli Studi di Pisa, Dipartimento di Chimica e Chimica Industriale,
Via Risorgimento 35, 56126 Pisa, Italy
Fax: + 39-0502219260
E-mail: gub@dcci.unipi.it
[b] CYCLOLAB Ltd.,
Illatos út 7, 1097 Budapest, Hungary
[c] Département de Recherche Fondamentale sur la Matière Condensée/Service de Chimie Inorganique et Biologique,
UMR-E no. 3, CEA-UJF/Laboratoire de Résonance Magnétique, CEA Grenoble,
17, Avenue des Martyrs, 38054, Grenoble Cedex 9, France
[d] Universität Tübingen, Institut für Organische Chemie,
Auf der Morgenstelle 18, 72076 Tübingen, Germany
Supporting information for this article is available on the WWW under http://www.eurjoc.org/ or from the author.

pound B" inside the cyclodextrin cavity and attractive fluorine–silicon interactions occurring at the external surface in enantiodiscrimination processes.[21]

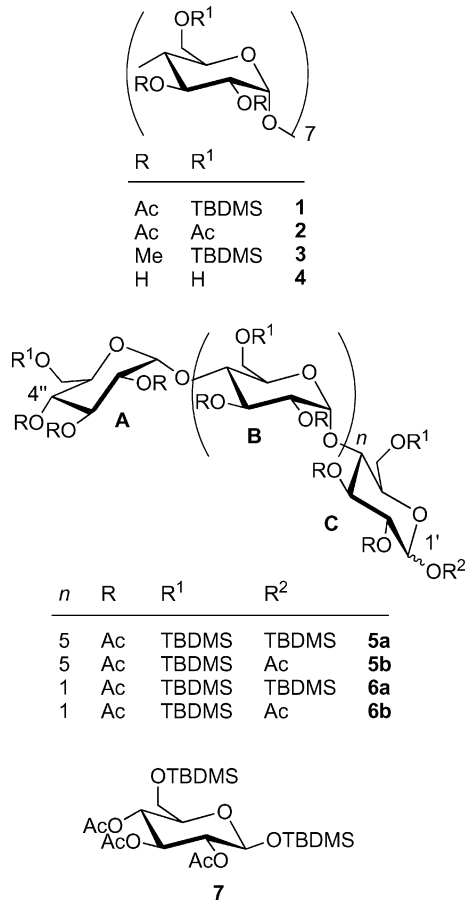

R	R^1	
Ac	TBDMS	**1**
Ac	Ac	**2**
Me	TBDMS	**3**
H	H	**4**

n	R	R^1	R^2	
5	Ac	TBDMS	TBDMS	**5a**
5	Ac	TBDMS	Ac	**5b**
1	Ac	TBDMS	TBDMS	**6a**
1	Ac	TBDMS	Ac	**6b**

Scheme 1. CSAs **1**–**7**.

Here, the use of the silylated-acetylated cyclodextrin **1** (Scheme 1) as a CSA for the NMR spectroscopic enantiodiscrimination of chiral fluorinated compounds possessing hydrogen-bond donor groups has been investigated in order to probe its versatility and to exploit the great potential of NMR spectroscopy for investigation of enantiodiscrimination processes at a molecular level, thereby complementing chromatographic approaches. Different kinds of α-amino acid derivatives were analysed (Scheme 2), focusing on *N*-trifluoroacetylated compounds **8**–**14** with free carboxy functions; the preparation of these compounds is very simple and purification is not required. In addition, compound **15**, with an ester function, and **16**, devoid of fluorine nuclei, were also examined. NMR analyses involved comparison of **1** with the peracetylated cyclodextrin **2** or the mixed methylated-silylated cyclodextrin **3** and the underivatized **4** (Scheme 1), in order to probe the relevance of the simultaneous presence of silyl and acetyl groups in the CSA. The role of the cavity of the cyclodextrin derivatives on enantiodiscrimination processes was investigated by comparison with the corresponding acyclic linear dextrin **5** (Scheme 1), which contains analogous derivatizing groups. Additionally, the linear dextrin **6**, with three glucopyranose units, and glucose derivative **7** (Scheme 1) were also probed. Investigations into the origin of enantiodiscrimination in solution involved extensive use of the DOSY (Diffusion Ordered SpectroscopY) technique[26–28] of measurement of translational diffusion coefficients, the potential of which in this field, mainly in the case of cyclodextrins chiral auxiliaries, has already been pointed out.[29–30]

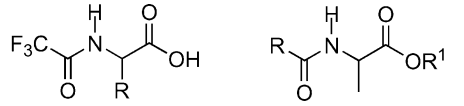

R		R	R^1	
CH_3	**8**	CF_3	CH_2CH_3	**15**
$CH_2CH_2SCH_3$	**9**	CH_3	H	**16**
*n*Pr	**10**			
*i*Pr	**11**			
*i*Bu	**12**			
Bn	**13**			
Ph	**14**			

Scheme 2. α-Amino acids derivatives **8**–**16**.

Results and Discussion

In enantiodiscrimination experiments, NMR spectra of pure racemic or enantiomerically enriched substrates **8**–**16** in $CDCl_3$ (Scheme 2) and their mixtures with selected chiral auxiliaries **1**–**7** (Scheme 1) were compared with each other. Typically, given the low solubility of α-amino acid derivatives, 5 mM solutions were analysed, even though the solubilities of the substrates increase up to 20 mM or higher in the mixtures with CSA **1**. In cases in which CSAs induced anisochrony of enantiotopic nuclei, then two sets of signals for each nucleus or group of equivalent nuclei of the two enantiomers were detected and nonequivalences ($|\delta_R - \delta_S|$, ppm) – differences of chemical shifts of corresponding nuclei in enantiomers (δ_R and δ_S) – could be measured. The magnitude of nonequivalence constitutes the more direct evidence of the efficiency of a CSA.

Starting our analysis from the racemic *N*-trifluoroacetyl derivative of alanine (**8**), we focused our attention on its amide resonance, which produces a signal in the high-frequency spectral region, not obscured by the CSAs' signals. The resonance of the amide proton of **8** was found as a broad singlet at $\delta = 6.86$ ppm, while in the presence of equimolar amounts of CSA **1** it was significantly split by 0.067 ppm (Table 1, Figure 1 a,b). The enantiomeric signals in the mixture were both significantly shifted to higher frequency than observed with the pure compound (7.07 ppm and 7.14 ppm; Table 1, Figure 1 a,b). The methine proton signals of **8**, which were obscured by the CSA signals, were extracted by COSY (COrrelation SpectroscopY) analysis and were found, also significantly split, at $\delta = 4.67$ ppm and 4.71 ppm (Supporting Information, Table S1). No doubling of the methyl resonances was observed. Amide proton nonequivalence, already high in the very low concentration (5 mM) equimolar mixture, showed a twofold increase with

increasing concentration to 10 mM and in the presence of two equivalents of CSA **1**, together with significant further higher-frequency shifts of enantiomeric signals (Table 1). The same effect of nonequivalence increase in methine protons was observed, but opposite complexation-induced chemical shifts (CICS, $\delta_{obs} - \delta_f$, ppm; δ_{obs} and δ_f are the chemical shifts of a selected nucleus in the presence and in the absence of the CSA, respectively) were detected in this case (see Table S1, Supporting Information).

Table 1. ^{1}H NMR (600 MHz, $CDCl_3$, 25 °C) CICSs ($\delta_{obs} - \delta_f$, ppm) and nonequivalences ($|\delta_R - \delta_S|$, ppm) of amide protons of **8**, **15** and **16** (5 mM) in the presence of equimolar amounts of CSA **1**.

Substrate	$\delta_{obs} - \delta_f$	$\lvert\delta_R - \delta_S\rvert$
8	0.277 (*S*)/0.210 (*R*)	0.067
8[a]	0.524 (*S*)/0.404 (*R*)	0.120
15	0.012	0
16	0.100	0

[a] At 10 mM in the presence of two equivalents of CSA.

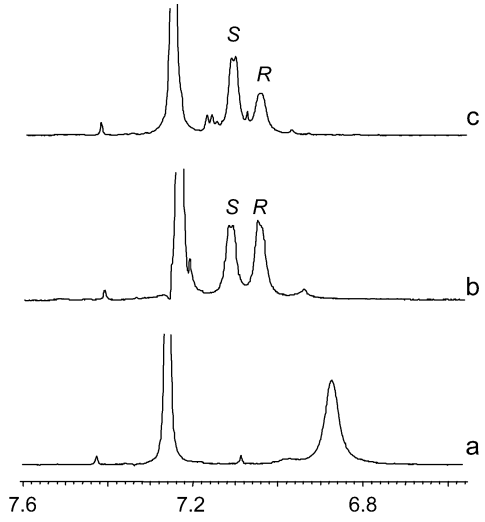

Figure 1. ^{1}H NMR (600 MHz, $CDCl_3$, 25 °C) spectra for regions corresponding to the amide proton of: a) **8** (5 mM), b) (*R*,*S*)-**8** (5 mM) in the presence of an equimolar amount of CSA **1**, and c) (*S*)-**8** (5 mM, enantiomeric purity 36%) in the presence of an equimolar amount of CSA **1**.

Under the same measurement conditions (5 mM, 1:1), no nonequivalence was detected in the analogous acetylated alanine derivative **16**, even though CICSs were also significantly high in this case (Table 1). The *N*-trifluoroacetylated alanine derivative **15**, with an ester function, showed both undetectable nonequivalence as well as significantly lower CICS of the amide proton. Consequently, the experiments involving derivatives **15** and **16** indicate that both fluorinated groups and free carboxyl functions are fundamental to achieving enantiodiscrimination of **8**–**14** by CSA **1**.

In consideration of the above results, *N*-trifluoroacetyl derivatives of different α-amino acids were analysed. All of them were efficiently enantiodiscriminated by **1**, with the exception of phenylglycine derivative **14** (Table 2). It is noteworthy that significant CICSs were also measured in this last case. Nonequivalences ranging from 0.067 ppm to 0.019 ppm were seen, with a maximum efficiency for alanine derivative **8** (Table 1) and methionine derivative **9** (Table 2).

Table 2. ^{1}H NMR (600 MHz, $CDCl_3$, 25 °C) CICSs ($\delta_{obs} - \delta_f$, ppm) and nonequivalences ($|\delta_R - \delta_S|$, ppm) of amide protons of **9**–**14** (5 mM) in the presence of equimolar amounts of CSA **1**.

Substrate	$\delta_{obs} - \delta_f$	$\lvert\delta_R - \delta_S\rvert$
9	0.199 (*S*)/0.137 (*R*)	0.062
10	0.152 (*S*)/0.133 (*R*)	0.019
11	0.109 (*S*)/0.084 (*R*)	0.025
12	0.162 (*S*)/0.141 (*R*)	0.021
13	0.132 (*S*)/0.110 (*R*)	0.022
14	0.226	0

The interesting point is that in all cases the investigated amide proton signal for the (*S*) enantiomer was shifted to higher frequency than the corresponding signal for the (*R*) enantiomer. The CSA **1** can thus also be proposed for configurational assignments of *N*-trifluoroacetylated derivatives of α-amino acids.

α-Amino acid derivative **8**, which was enantiodiscriminated with very high efficiency by CSA **1**, was employed as an enantiomeric substrate for enantiodiscrimination experiments with the different CSAs **2**–**7** (Tables 3 and 4).

In particular, peracetylated cyclodextrin **2**, devoid of silyl functionalities, produced significantly lower differentiation of the amide proton in **8** (0.020 ppm, Table 3), but CICSs were high, although lower than they had been in the presence of CSA **1**. Cyclodextrin **3**, silylated like **1** on its primary sites but methylated, rather than acetylated, on its secondary ones, did not produce any differentiation of enantiomeric signals and produced lower CICSs (Table 3). Interestingly, CICSs produced by **1** nearly corresponded to the sums of measured CICSs in the presence of cyclodextrins **2** and **3** (Tables 1 and 3).

Table 3. ^{1}H NMR (600 MHz, $CDCl_3$, 25 °C) CICSs ($\delta_{obs} - \delta_f$, ppm) and nonequivalences ($|\delta_R - \delta_S|$, ppm) of the amide proton in **8** (5 mM) in the presence of equimolar amounts of CSAs **2**–**3**.

CSA	$\delta_{obs} - \delta_f$	$\lvert\delta_R - \delta_S\rvert$
2	0.190 (*S*)/0.170 (*R*)	0.020
3	0.087	0
2 + **3**	0.251 (*S*)/0.240 (*R*)	0.011

A ternary mixture containing **8** in the presence of both **2** and **3** was then analysed, giving CICSs as high as in the equimolar **8**/**1** mixture, while nonequivalence was significantly lower (Table 3). This result shows the role of both silyl and acetyl groups in the stabilization of diastereomeric solvates formed in solution. Enantiodiscrimination must, however, result from a cooperative action of the two functionalities in the CSA **1**.

Further verification of the relevance of derivatizing groups in enantiodiscrimination processes was provided by comparison with underivatized β-cyclodextrin **4**, employed in D_2O because of its very low solubility in $CDCl_3$. H–D exchange of the amide proton of **8** occurring in D_2O prevented its observation, so analysis was based on the meth-

ine proton, which had also been differentiated in the previously discussed mixtures. The above signal did not undergo any doubling as the consequence of the presence of **4** and nor did it give detectable CICSs, suggesting that significant CSA–solute interaction did not occur.

With regard to comparison with the linear acyclic derivatized oligosaccharides **5**–**7** (Table 4), the two kinds of products, either silylated (**a**) at the anomeric carbon or acetylated (**b**) on it (Scheme 1), behaved indistinguishably in enantiodiscrimination experiments (Table 4). The influence of the nature of the functional group on the anomeric centre (TBDMS vs. acetyl) was also tested by gas chromatographic experiments, with no significant differences in the enantioseparation being observed.

Table 4. ^{1}H NMR (600 MHz, $CDCl_3$, 25 °C) CICSs ($\delta_{obs} - \delta_f$, ppm) of amide proton of **8** (5 and 10 mM) in the presence of one or two equivalents of CSAs **5**–**7**.

CSA	5 mM, 1:1 $\delta_{obs} - \delta_f$	10 mM, 1:2 $\delta_{obs} - \delta_f$
5a	0.113	0.223 (*S*)/0.204 (*R*)
5b	0.114	0.223 (*S*)/0.204 (*R*)
6a	0.061	0.131
6b	0.059	0.129
7	0.041	0.056

Once again, we selected alanine derivative **8** as the enantiodiscrimination probe compound and found that at 5 mM no acyclic oligosaccharide was able to differentiate its enantiomers (Table 4). Only **5a**–**b**, with seven glucopyranose units, produced nonequivalence, of about 0.020 ppm (Table 4, Figure 2) in mixtures containing 10 mM **8** in the presence of two equivalents of **5a** or **5b**. Under the same experimental conditions neither of the oligosaccharides **6**–**7** allowed the observation of differentiated signals of the enantiomers of **8** (Table 4). Analysis of CICSs by **5**–**7** revealed several interesting aspects: CSAs **5a**–**b** were unable to enantiodiscriminate **8** at 5 mM, but caused significant high-frequency shifts (0.11 ppm) of its amide resonance (Table 4). Trisaccharide **6** also caused a high-frequency shift (0.060 ppm), about half of that measured for **5**, and an even more lower CICS was measured in the presence of monosaccharide **7** (Table 4).

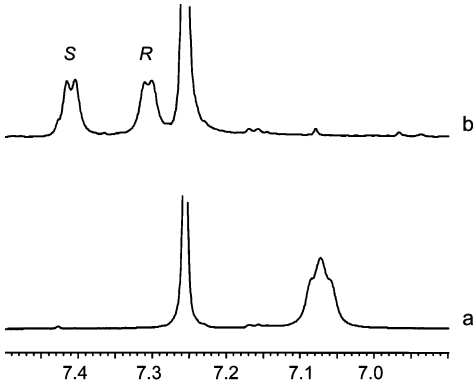

Figure 2. ^{1}H NMR (600 MHz, $CDCl_3$, 25 °C) spectral regions corresponding to the amide proton of **8** (10 mM) in the presence of two equivalents of CSA: a) **5a**–**b**, b) **1**.

The complexing abilities of acyclic oligosaccharides thus mainly depend on the number of glucopyranose units, but efficient enantiodiscrimination requires the concatenation of glucopyranose units by a cyclic assembly, which may suggest the occurrence of inclusion processes. However, if we take into account that all acyclic oligosaccharides are able to give rise to complexation phenomena with **8**, but that this brought about enantiodiscrimination only in the case of **5a**–**b**, we must consider the alternative hypothesis that the rigid structure generated by cyclic assembly is responsible for enantiodiscrimination as the consequence of spatial constraints imposed by silyl and acetyl moieties on the primary and secondary sites, respectively, of adjacent units.

To obtain deeper insight into these aspects, NMR DOSY experiments were carried out. DOSY techniques[26–28] make it possible to detect translational molecular diffusion by measurement of the diffusion coefficient (D). From the Stokes–Einstein equation [Equation (1)] the diffusion coefficient can be correlated to friction factor f, where k is the Boltzmann constant and T the absolute temperature.

$$D = \frac{kT}{f} \quad (1)$$

The friction factor of spherical molecules can be correlated to molecular size by means of the hydrodynamic radius R_H [Equation (2)], where η is solution viscosity and c represents a numerical factor that for medium- to large-sized molecules is approximately 6, whereas for molecules with sizes comparable to those of the solvent it can be estimated from a semiempirical improvement[31–33] of the equation derived from the theory proposed by Wirtz and coworkers.[34,35]

$$f = c\pi\eta R_H \quad (2)$$

The following special comment on the dependence of the diffusion coefficient on solution viscosity is appropriate. For dilute solutions it is approximately equal to solvent viscosity, but in all other cases an internal standard of viscosity must be employed. To this end, in organic solvents, tetramethylsilane (TMS) can be employed.[36] Its diffusion coefficients in the presence and in the absence of substrate can be measured and their ratio employed as a viscosity correction factor.

In any case, the dependence of diffusion coefficients on the hydrodynamics radii makes these parameters a powerful probe for complexation phenomena, which always cause increases in molecular size and hence bring about decreases in diffusion coefficients measured by the DOSY technique. In particular, under fast-exchange conditions (i.e., when diffusion of free and complexed species are indistinguishable), the measured diffusion coefficient (D_{obs}) represents the weighted average of the value corresponding to the uncomplexed (D_f) and complexed (D_c) forms [Equation (3)], where

x_f and x_c are the molar fractions of uncomplexed and complexed forms, respectively, with $x_f + x_c = 1$.

$$D_{obs} = D_f x_f + D_c x_c \quad (3)$$

From Equation (3), the magnitude of the decrease in the diffusion coefficient, occurring as the consequence of complexation processes, is correlated to complexed molar fraction x_c [Equation (4)] and, hence, to complexation constant K.

$$x_c = \frac{D_{obs} - D_f}{D_c - D_f} \quad (4)$$

Although, in the fast exchange regime, the same relationship also applies to other averaged NMR parameters, such as chemical shifts, coupling constants or relaxation rates, we would point out that diffusion coefficients are particularly suitable for complexation investigations, as they represent global parameters of the molecule as a whole and not local parameters. Furthermore, when we deal with diastereomeric complexes such as those formed with the use of CSAs, it is reasonable to hypothesize that the diffusion coefficients of the two complexed enantiomers (D_c^R and D_c^S) are equal, unless complexation stoichiometry changes. The above approximation can never be made for local parameters strongly affected by stereochemical factors.

Thus, the ratios of complexed molar fractions of the enantiomers can be very simply determined [Equation (5)].

$$\frac{x_c^R}{x_c^S} = \frac{D_{obs}^R - D_f}{D_{obs}^S - D_f} \quad (5)$$

Furthermore, when enantiomeric substrates and CSAs are of significantly different sizes, it can be assumed that translational diffusion is mainly controlled by the larger molecule, frequently the CSA, and, hence, that the diffusion coefficient of enantiomeric substrates in the complexed states (D_c^R and D_c^S) are approximately equal to the CSA diffusion coefficient (D_{CSA}).[21,29,30]

In this way, by single-point determinations, the complexed molar fraction at a single concentration value can be determined as in Equation (6), and from this the complexation constant K can be calculated. This approach proved to be very useful, above all in the case of cyclodextrin CSAs.[21,29,30]

$$x_c = \frac{D_{obs} - D_f}{D_{CSA} - D_f} \quad (6)$$

Finally we would point out that comparison between CICSs ($\Delta\delta$) and complexation-induced variation of diffusion coefficients (ΔD) is a powerful tool for identifying the origin of enantiodiscrimination. On the basis of Equation (3) and Equation (7), detection of differentiated diffusion coefficients of the two enantiomers necessarily involves differentiated complexed molar fractions [Equation (3)] and, hence, complexation constants, whereas strongly differentiated complexation-induced variation of chemical shifts can be caused both by differences in enantiomer-complexed molar fractions as well as by differences in their stereochemical arrangements ($\delta_c^R \neq \delta_c^S$) [Equation (7)]. On this basis, we measured the diffusion coefficients of enantiomers of **8** both pure and in the presence of selected CSAs, under different experimental conditions.

$$\delta_{obs} = \delta_f x_f + \delta_c x_c \quad (7)$$

In each case TMS (1%) was employed as internal standard of viscosity, and measured diffusion coefficients were corrected as already stated. Such a correction was mainly needed for solutions of high CSA concentration. As an example, for a 1 mM $CDCl_3$ solution of the cyclodextrin we measured a diffusion coefficient of CSA **1** equal to 4.4×10^{-10} m^2 s^{-1} and for TMS equal to 21.0×10^{-10} m^2 s^{-1}. Already at 5 mM, the diffusion coefficient of **1** had decreased to 4.3×10^{-10} m^2 s^{-1}, and at the maximum concentration of 40 mM the diffusion coefficient of CSA **1** had become 3.5×10^{-10} m^2 s^{-1}, while the corresponding diffusion coefficients for TMS were 20.6×10^{-10} m^2 s^{-1} and 17.4×10^{-10} m^2 s^{-1} (Supporting Information, Table S2). The corrected values of the diffusion coefficients of cyclodextrin **1** are always 4.4×10^{-10} m^2 s^{-1}, demonstrating that measured variations are only due to viscosity changes and not to a self-aggregation phenomenon.

We thus first measured the diffusion coefficient of (*R*)- and (*S*)-**8**/CSA **1** equimolar mixtures at the 5 mM total concentration and measured diffusion coefficients (corrected for viscosity changes) of 10.7×10^{-10} m^2 s^{-1} and 11.8×10^{-10} m^2 s^{-1} for (*S*)- and (*R*)-**8**, respectively. Thus, from Equation (6), we calculated complexed molar fractions of 0.21 for (*S*)-**8** and 0.08 for (*R*)-**8**, which gave complexation constants of 67 M^{-1} and 19 M^{-1}, respectively (Table 5, Figure 3).

Table 5. Diffusion coefficients[a] ($D \times 10^{10}$ m^2 s^{-1}, 600 MHz, $CDCl_3$, 25 °C) of α-amino acid derivatives **8**–**14** (5 mM) in the absence (D_f) and in the presence (D_{obs}) of CSA **1**.

Substrate	D_f	D_{obs}
8	12.4	10.7 (*S*)/11.8 (*R*)
9	10.5	8.4 (*S*)/9.1 (*R*)
10	11.0	10.3
11	11.3	10.5
12	10.7	10.2
13	10.4	9.5
14	10.6	9.6

[a] Corrected employed TMS as internal standard.

However, the same kind of analysis performed in a solution containing (*R*)- or (*S*)-**8** at a significantly lower concentration (1 mM) in the presence of a tenfold CSA molar excess gave significantly different complexation constants of 89 M^{-1} and 66 M^{-1} for (*S*)- and (*R*)-**8**, respectively (Table 6). This remarkable discrepancy can be attributed to the fact that *N*-trifluoroacetyl derivatives of α-amino acids with free carboxyl functions strongly self-aggregate in solution, as

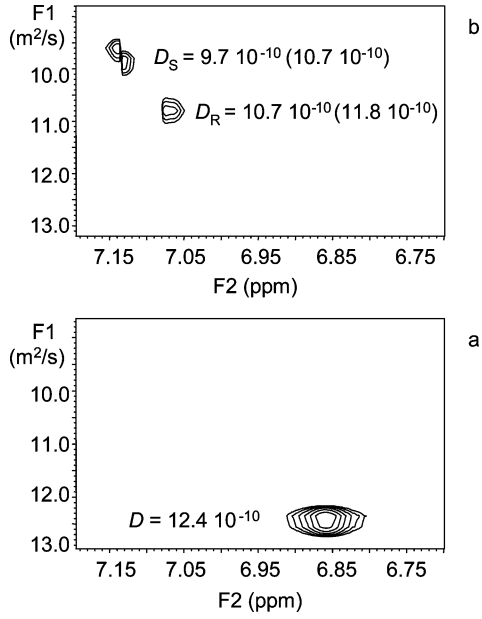

Figure 3. DOSY (600 MHz, $CDCl_3$, 25 °C) maps of **8** (5 mM) in the absence (a) and in the presence (b) of an equimolar amount of CSA **1**. Viscosity corrected values are reported in parentheses.

demonstrated by analysis of progressively diluted solutions [as an example for **8**, D (5 mM) = 12.4×10^{-10} $m^2 s^{-1}$ and D (1 mM) = 13.6×10^{-10} $m^2 s^{-1}$]. Hence, in the evaluation of complexation constants only experimental conditions discouraging self-aggregation processes in comparison with heteroassociation phenomena (i.e., low concentrations of the self-aggregating species in the presence of high molecular excesses of a species that does not tend to self-aggregate) should be employed, as in the case we have just described.

Table 6. Diffusion coefficients[a] ($D_{obs} \times 10^{10}$ $m^2 s^{-1}$, 600 MHz, $CDCl_3$, 25 °C) of enantiomers of **8** (5 mM) in the presence of CSA **1**, and complexation constants (K, M^{-1}).

Substrate	[**8**] [mM]	**8**/**1**	D_{obs}	K[b]
(*S*)-**8**	5	1:1	10.7	67 ± 5 (90 ± 4)
(*R*)-**8**	5	1:1	11.8	19 ± 5 (57 ± 4)
(*S*)-**8**	1	1:10	9.4	89 ± 5 (90 ± 4)
(*R*)-**8**	1	1:10	10.0	66 ± 8 (57 ± 4)

[a] Corrected by use of TMS as internal standard. [b] Association constants determined by the Foster–Fyfe method[37,38] (concentration of **8** 1 mM) are reported in parenthesis.

To confirm the validity of our approach we verified the hypothesis of 1:1 stoichiometry by Job's method and then determined the association constants of the two diastereomeric complexes by the Foster–Fyfe method,[29,37,38] by analysing 1 mM (*R*)- or (*S*)-**8** solutions in the presence of increasing molar excesses of CSA **1** from 1:20 to 1:140 (see Table S3, Figure S1 in the Supporting Information). By linear fitting of experimental data, we calculated the two values of complexation constants of 90 M^{-1} and 57 M^{-1} for (*S*)- and (*R*)-**8**, respectively, and these were in very good agreement with the values obtained from diffusion coefficient measurements by the single-point method in the 1:10 substrate/CSA solution (Table 6).

Returning to the main goal of our investigation, we can conclude, not only because the CICSs are highly and significantly differentiated, but also because the diffusion coefficients underwent significantly different decreases due to complexation to CSA, that cyclodextrin **1** is able to enantiodiscriminate the enantiomers of **8** through the formation of diastereomeric complexes that are significantly distinct with regard not only to their stereochemistry, but also to their thermodynamic stability.

Analogous DOSY and chemical shift measurements in mixtures containing the other α-amino acid derivatives demonstrated the ability of cyclodextrin **1** to produce decreases in the diffusion coefficients of enantiomeric substrates, which are differentiated only in the cases of the previously discussed alanine derivative and the methionine one (Table 5). Accordingly, nonequivalences (Table 2) were significantly higher for **8**–**9** than for **10**–**14**, thus showing that the more efficient enantiodiscrimination occurs when the CSA is able to differentiate not only the stereochemical environments of the enantiomers, but also their complexation constants.

The variations in the undifferentiated diffusion coefficients of (*S*)- and (*R*)-**8** due to the presence of equimolar amounts of cyclodextrins **2** and **3** were 10.7×10^{-10} $m^2 s^{-1}$ [i.e., equal to that observed for the more tightly bound enantiomers [(*S*)-**8**] in the presence of CSA **1** (Table 5)], confirming the roles of acetyl and silyl groups in the stabilization of the complexes formed in solution. However, at least in the case of **2**, observed nonequivalence is mainly due to the fact that the two diastereoisomers have different stereochemistry in solution, while their complexation constants are not significantly different. Silyl groups must be mainly involved in the stabilization of the diastereomeric complexes, but alone are not able to differentiate enantiomers' environments, precluding any differentiation from the thermodynamic point of view.

Acyclic linear oligosaccharides did not produce any differentiation of the diffusion coefficients of the enantiomers, and the magnitude of their decrease (Table 7) is strongly dependent on the number of glucopyranose units, confirming previously discussed results regarding CICSs (Table 4).

Table 7. Diffusion coefficients[a] ($D_{obs} \times 10^{10}$ $m^2 s^{-1}$, 600 MHz, $CDCl_3$, 25 °C) of α-amino acid derivative **8** (5 mM) in the presence of equimolar amounts of CSAs **5**–**7**.

	5a	**5b**	**6a**	**6b**	**7**
D_{obs}	11.7	11.7	12.1	12.1	12.4

[a] Corrected by employing TMS as internal standard.

In the presence of the heptasaccharides **5a** and **5b** a decrease in the diffusion coefficient of both enantiomers to 11.7×10^{-10} $m^2 s^{-1}$ is detected, which is comparable to the effect produced by CSA **1** on the less tightly complexed (*R*) enantiomer (Table 5). The effect of tri- and monosaccharides on the diffusion coefficients of **8** are almost negligible, demonstrating that the number of units strongly affects the ability of CSA to stabilize complexes formed in solution. Complexation constants for trisaccharides **6** and heptasac-

charides **5** were also determined by the Foster–Fyfe method,[37,38] giving values of 32 M^{-1} and 62 M^{-1}, respectively (see Table S4, Figure S2, Supporting Information). It is noteworthy that this last value is very similar to the complexation constant measured for (*R*)-**8** in the presence of CSA **1**. Thus, we can conclude that the ability of oligosaccharides to stabilize enantiomeric mixtures through the formation of diastereomeric complexes is less pronounced than it is in the case of cyclic oligosaccharides and strongly depends on the number of glucopyranose rings. In any case, even though the heptasaccharide CSA is itself able to complex enantiomeric mixtures, it is not able to differentiate their stereochemical environments significantly.

To conclude our analysis, we carried out ROE (Rotating-frame Overhauser Enhancement) measurements of intermolecular dipolar interactions in mixtures containing (*S*)- or (*R*)-**8** at 1 mM concentrations in the presence of ten equivalent of cyclodextrin **1** in order to obtain some information on proximity constraints inside diastereomeric complexes. The above experimental conditions were selected in order to guarantee an approx. 40% complexed molar fraction in solution.

Perturbation of the external proton H^1 in CSA **1** (Figure 4) produced the expected intra-unit H^1–H^2 effect and the inter-unit H^1–H^4 effect, in addition to significant effects on the H^3 and H^5 internal protons, which must be due to glucopyranose units tilting about glycosidic linkages (see Figure S3, Supporting Information).

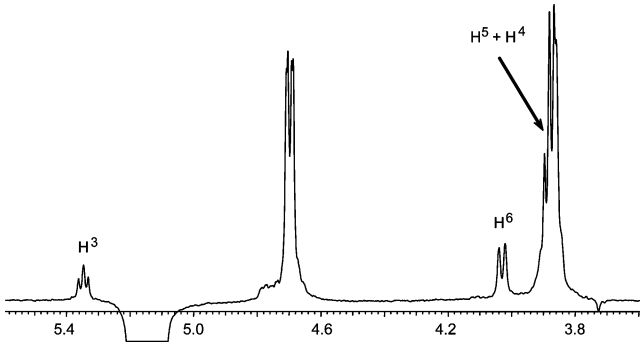

Figure 4. 1D ROESY (600 MHz, $CDCl_3$, 25 °C, mix 0.9 s) spectrum corresponding to perturbation of the H^1 protons in CSA **1**.

Acetyl protons of groups bound to secondary sites produced clear dipolar interaction with protons of *tert*-butyldimethylsilyl groups, demonstrating that both kinds of groups face the external surface of the cyclodextrin (Figure 5). Their proximity is probably favoured by tilted glucopyranose rings. Interestingly, significant dipolar interaction between the acetyl functions of the cyclodextrin and the methyl groups of both enantiomers of **8** was also detected (Figure 5). The reciprocal effect was also detected in the 1D ROESY spectrum obtained by perturbation of methyl protons of (*S*)- or (*R*)-**8** (Figure 6), while further effects were found at the silyl frequencies and on the external proton H^2. It is noteworthy that a smaller effect on the internal proton H^3 was also detected. As this last effect is less pronounced than effects detected on external protons, we can

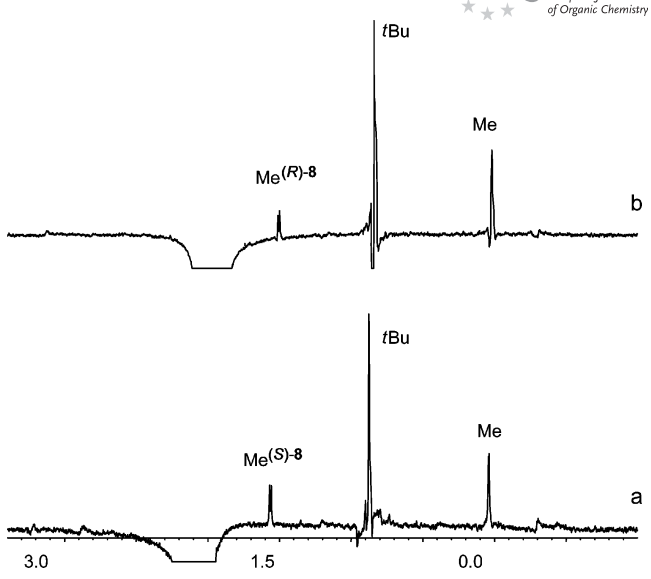

Figure 5. 1D ROESY (600 MHz, $CDCl_3$, 25 °C, mix 0.9 s) spectra corresponding to perturbation of acetyl protons of CSA **1** in equimolar mixture: a) (*S*)-**8**/**1**, b) (*R*)-**8**/**1**.

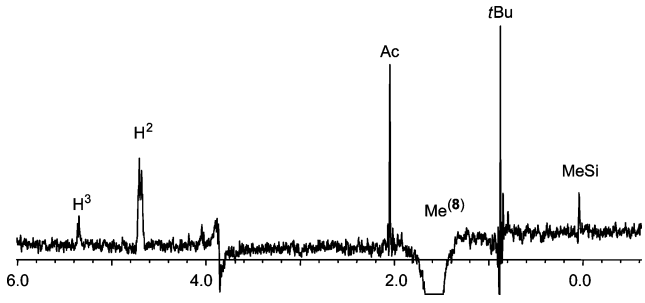

Figure 6. 1D ROESY (600 MHz, $CDCl_3$, 25 °C, mix 0.9 s) spectrum corresponding to perturbation of methyl protons of **8** in an equimolar (*S*)-**8**/**1** mixture.

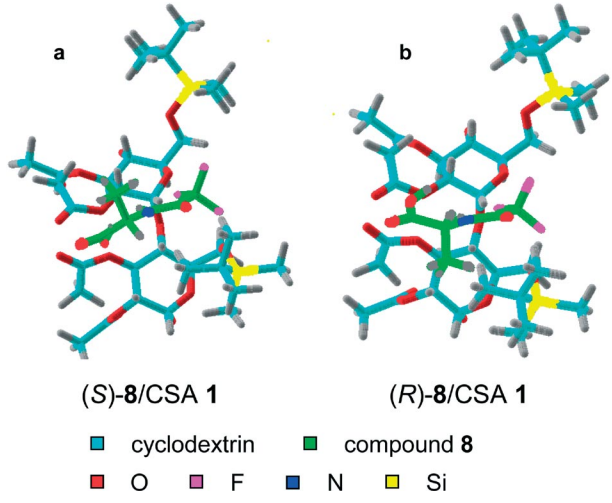

Figure 7. Graphical representation of diastereomeric complexes (*S*)-**8**/**1** (a) and (*R*)-**8**/**1** (b). Only two glucopyranose units of CSA **1** are represented.

conclude that complexation occurs at the external surface of the cyclodextrin and that the effect detected on the internal proton H^3 is mainly due to the rotation of CSA **1** units, which brings internal protons H^3 into the vicinity of the external surface of the cyclodextrin (Figure 7).

Conclusions

The mixed silylated-acetylated β-cyclodextrin **1** is an efficient CSA for direct determinations of enantiomeric purities of fluorinated α-amino acid derivatives by NMR spectroscopy. Interestingly, regular correlations found between relative positions of enantiomers' amide resonances and absolute configuration also suggested the potential to employ CSA **1** for configurational assignments of the same class of α-amino acid derivatives. Therefore, an analytical NMR approach complementary to the GC use of CSA **1** can be suggested, significantly extending the potential application of the CSA.

In the NMR enantiodiscrimination of simple *N*-trifluoroacetyl derivatives of α-amino acids by CSA **1**, the importance of the presence of fluorinated groups and free carboxyl functions in the enantiomeric substrates has been identified. Both silyl and acetyl groups in the CSA are involved in the stabilization of diastereomeric complexes, but only their simultaneous presence brings about efficient enantiodiscrimination. Acyclic linear oligosaccharides made up of seven, three and one glucopyranose units are also able to complex enantiomeric substrates preferentially, and the amount of complexation strongly depends on the number of glucopyranose units. A cyclic assembly of glucopyranose rings gives rise to a rigid structure, probably allowing attractive fluorine–silicon interactions, which could be assisted by attractive interactions involving the carboxyl functions of α-amino acids and acetyl moieties of the CSA. The cooperation of these attractive interactions reasonably orients the complexation of the enantiomeric substrates at the external surface of cyclodextrin rather than inside its cavity. Accordingly, the acyclic linear heptasaccharide is also able to bring about enantiodiscrimination, but differentiates enantiomers to a smaller extent than CSA **1**, which is probably due to its less rigid structure.

Experimental Section

General Methods: NMR measurements were performed on a spectrometer operating at 600 and 150 MHz for ^1H and ^{13}C, respectively. The temperature was controlled to ±0.1 °C. ^1H and ^{13}C NMR chemical shifts are referenced to TMS as external standard. The 2D NMR spectra were obtained by using standard sequences. Proton gCOSY 2D spectra were recorded in the absolute mode with acquisition of four scans with a 5 s relaxation delay between acquisitions for each of 256 FIDs. Proton 1D ROESY spectra were recorded by using selective pulses generated by means of the Varian Pandora Software. The 1D ROESY spectra were acquired with 256–1024 scans in 32 K data points with a 5 s relaxation delay and a mixing time of 0.9 s. 2D TOCSY (TOtally Correlation SpectroscopY) spectra were recorded by employing a mixing time of 65 ms. The pulse delay was maintained at 5 s; 256 increments of eight scans and 2 K data points each were collected. The data matrix was zero-filled to 2 K × 1 K and sinebell and sinebell shifted functions were applied for processing in both dimensions. Proton 1D TOCSY spectra were recorded by using selective pulses generated by means of the Varian Pandora Software. The 1D TOCSY spectra were acquired with 256–1024 scans in 32 K data points with a 5 s relaxation delay and a mixing time ranging from 60 to 120 ms. The gradient ^1H,^{13}C-gHSQC (gradient Heteronuclear Single Quantum Correlation) spectra were obtained in 16 transients per increment into a 2048 × 128 point data matrix. The gradient HMBC (Heteronuclear Multiple Bond Correlation) experiments were optimized for a long-range ^1H–^{13}C coupling constant of 8 Hz. The spectra were acquired with 256 time increments, 16 scans per t_1 increment and a 3.5 ms delay period for suppression of one-bond correlation signals. No decoupling during acquisition was used. DOSY experiments were carried out by using a stimulated echo sequence with self-compensating gradient schemes, a spectral width of 7000 Hz and 64 K data points. Typically, a value ranging from 50 to 190 ms was used for Δ, 1.0 ms for δ, and g was varied in 30 steps (16 transients each) to obtain an approximately 90–95% decrease in the resonance intensity at the largest gradient amplitudes. The baselines of all arrayed spectra were corrected prior to processing of the data. After data acquisition, each FID was apodized with 1.0 Hz line broadening and Fourier-transformed. The data were processed with the DOSY macro (involving the determination of the resonance heights of all the signals above a pre-established threshold and the fitting of the decay curve for each resonance to a Gaussian function) to provide pseudo two-dimensional spectra with NMR chemical shifts along one axis and calculated diffusion coefficients along the other.

Materials: Heptakis[2,3-di-*O*-acetyl-6-*O*-(*tert*-butyldimethylsilyl)]-β-cyclodextrin (**1**) and heptakis[6-*O*-(*tert*-butyldimethylsilyl)-2,3-di-*O*-methyl]-β-cyclodextrin (**3**) were prepared according to literature procedures[39,40] and the ^1H and ^{13}C NMR were in accordance with those previously reported.[41] Compounds **5**–**7** were synthesized as already described elsewhere.[24,25] *N*-Trifluoroacetyl derivatives[42] of α-amino acids **8**–**14** and *N*-(trifluoroacetyl)alanine ethyl ester (**15**)[43] were synthesized as described elsewhere.

Maltoheptaose 5a: ^1H NMR (600 MHz, $CDCl_3$, 25 °C): δ = –0.07–0.15 (48 H, Me), 0.73–0.95 (72 H, *t*Bu), 1.91–2.21 (45 H, Me, Ac), 3.40–4.01 (H^6, H^5, H^{4A}, H^{4B}), 4.59–4.80 (H^2, H^{1A}), 5.18 (H^{4C}), 5.20–5.40 (H^3, H^{1B}, H^{1C}) ppm. ^{13}C NMR (150 MHz, $CDCl_3$, 25 °C): δ = –5.7 to –4.2 [$(CH_3)_2Si$], 17.8, 18.3, 18.4, 18.5 [$(CH_3)_3C$], 20.2–21.4 (CH_3, Ac), 25.1–26.2 [$(CH_3)_3C$], 60.8–61.8 (C^6), 68.1–75.4 (C^2, C^3, C^4, C^5), 94.4–95.9 (C^1) 169.1–170.7 (CO, Ac) ppm.

Maltoheptaose 5b: ^1H NMR (600 MHz, $CDCl_3$, 25 °C): δ = –0.04–1.11 (42 H, Me), 0.74–0.94 (63 H, *t*Bu), 1.93–2.21 (48 H, Me, Ac), 3.53 ($H^{5A}{}_\beta$), 3.70–4.03 ($H^{66'}$), 3.82 ($H^{5A}{}_\alpha$), 3.88 (H^{5C}), 3.90 (H^{4B}, H^{5B}) 4.01 ($H^{4A}{}_\alpha$) 4.03 ($H^{4A}{}_\beta$), 4.63 (H^{2B}), 4.78 (H^{2C}), 4.89 ($H^{2A}{}_\alpha$), 4.91 ($H^{2A}{}_\beta$), 5.18 (H^{4C}), 5.26 (H^{1B}), 5.28 ($H^{3A}{}_\beta$), 5.30 (H^{3C}), 5.35 (H^{3B}), 5.37 (H^{1C}), 5.49 ($H^{3A}{}_\alpha$), 5.68 (d, $J_{1,2}$ = 8.3 Hz, $H^{1A}{}_\beta$), 6.22 (d, $J_{1,2}$ = 3.8 Hz, $H^{1A}{}_\alpha$) ppm. ^{13}C NMR (150 MHz, $CDCl_3$, 25 °C): δ = –5.7 to –4.8, [$(CH_3)_2Si$], 18.2–18.6 [$(CH_3)_3C$], 20.3-21.2 (CH_3, Ac), 25.8–26.2 [$(CH_3)_3C$], 61.1–61.8 (C^6), 68.1 (C^{4C}), 69.7–72.6 (C^2, C^3, C^4, C^5), 89.2 ($C^{1A}{}_\alpha$), 91.5 ($C^{1A}{}_\beta$), 95.6–95.9 (C^1), 169.0–170.8 (CO-Ac) ppm.

Maltotriaose 6a: ^1H NMR (600 MHz, $CDCl_3$, 25 °C): δ = –0.05 to 0.13 (24 H, Me), 0.75 to 0.95 (36 H, *t*Bu), 1.92–2.20 (21 H, Me, Ac), 3.40 (H^{5A}), 3.63 ($H^{6'C}$), 3.71 (H^{6C}), 3.81 ($H^{6'B}$), 3.87 (H^{5C}), 3.91 (H^{6B}), 3.93 (H^{4A}, $H^{66'A}$), 3.97 (H^{4B}), 3.99 (H^{5B}), 4.61 (H^{2B}), 4.72 (H^{1A}, H^{2A}), 4.77 (H^{2C}), 5.16 (H^{4C}), 5.22 (H^{3A}), 5.26 (H^{1B}), 5.32 (H^{1C}, H^{3C}), 5.36 (H^{3B}) ppm. ^{13}C NMR (150 MHz, $CDCl_3$, 25 °C): δ = –5.9 to –4.7 [$(CH_3)_2Si$], 18.0–18.8 [$(CH_3)_3C$], 20.3-21.2

(CH_3, Ac), 25.1–26.4 [(CH_3)$_3$C], 61.3 (C^{6C}), 61.9 (C^{6B}), 62.2 (C^{6A}), 68.1 (C^{4C}), 69.4 (C^{5B}), 70.2 (C^{3C}), 70.3 (C^{5C}), 70.6 (C^{2C}), 71.1 (C^{2B}), 71.2 (C^{4B}), 71.7 (C^{3B}), 72.3 (C^{4A}), 74.1 (C^{2A}), 75.0 (C^{3A}), 75.4 (C^{5A}), 94.9 (C^{1C}), 95.1 (C^{1B}), 95.2 (C^{1A}) 169.2, 169.6, 169.8, 170.1, 170.3, 170.4, 170.5 (CO, Ac) ppm.

Maltotriaose 6b: ^{1}H NMR (600 MHz, $CDCl_3$, 25 °C): δ = –0.01 to 0.10 (18 H, Me), 0.84–0.94 (27 H, *t*Bu), 1.95–2.23 (24 H, Me, Ac), 3.52 (d, $J_{5,4}$ = 9.7 Hz, $H^{5A}{}_\beta$), 3.64 ($H^{6'C}$), 3.72 (H^{6C}), 3.74 ($H^{6'B}$), 3.80 (H^{6B}), 3.81 ($H^{5A}{}_\alpha$), 3.86 (H^{5C}), 3.89 ($H^{6'A}{}_\beta$), 3.95 ($H^{6A}{}_\beta$), 3.98 (H^{5B}), 3.99 ($H^{4A}{}_\alpha$, $H^{4A}{}_\beta$, H^{4B}, $H^{66'A}{}_\alpha$), 4.62 (dd, $J_{2,3}$ = 10.8, $J_{2,1}$ = 3.7 Hz, $H^{2B}{}_\beta$), 4.63 (dd, $J_{2,3}$ = 10.8, $J_{2,1}$ = 3.7 Hz, $H^{2B}{}_\alpha$), 4.77 (dd, $J_{2,3}$ = 10.4, $J_{2,1}$ = 3.7 Hz, H^{2C}), 4.90 (dd, $J_{2,3}$ = 10.1, $J_{2,1}$ = 3.8 Hz, $H^{2A}{}_\alpha$), 4.92 (dd, $J_{2,3}$ = 9.7, $J_{2,1}$ = 8.3 Hz, $H^{2A}{}_\beta$), 5.16 (t, $J_{4,3}$ = $J_{4,5}$ = 10.4 Hz, H^{4C}), 5.27 (H^{1B}), 5.29 ($H^{3A}{}_\beta$), 5.33 (H^{3C}), 5.38 (H^{1C}), 5.39 (H^{3B}), 5.51 (t, $J_{3,2}$ = $J_{3,4}$ = 10.1 Hz, $H^{3A}{}_\alpha$), 5.68 (d, $J_{1,2}$ = 8.3 Hz, $H^{1A}{}_\beta$), 6.25 (d, $J_{1,2}$ = 3.8 Hz, $H^{1A}{}_\alpha$) ppm. ^{13}C NMR (150 MHz, $CDCl_3$, 25 °C): δ = di M_1 –5.7 to –4.8, [(CH_3)$_2$Si], 18.2–18.5 [(CH_3)$_3$*C*], 20.5–21.0 (CH_3, Ac), 25.8 [(CH$_3$)$_3$C], 25.9 [2×(CH$_3$)$_3$C], 61.3 ($C^{6B}{}_\beta$), 61.4 ($C^{6B}{}_\alpha$), 61.5 ($C^{6C}{}_\alpha$), 61.7 ($C^{6A}{}_\beta$), 61.8 ($C^{6C}{}_\beta$), 61.8 ($C^{6A}{}_\alpha$), 68.0–75.9 (C^2, C^3, C^4, C^5), 89.2 ($C^{1A}{}_\alpha$), 91.5 ($C^{1A}{}_\beta$), 94.8 ($C^{1C}{}_\alpha$), 94.9 ($C^{1C}{}_\beta$), 95.3 ($C^{1B}{}_\beta$), 95.4 ($C^{1B}{}_\alpha$), 168.9–170.5 (CO, Ac) ppm.

2,3,4-Tri-*O*-acetyl-1,6-di-*O*-(*tert*-butyldimethylsilyl)-D-glucose (7): ^{1}H NMR (600 MHz, $CDCl_3$, 25 °C): δ = 0.03 (s, 3 H, Me-6), 0.04 (s, 3 H, Me-6), 0.10 (s, 3 H, Me-1), 0.12 (s, 3 H, Me-1), 0.86 (s, 9 H, *t*Bu-1), 0.88 (s, 9 H, *t*Bu-6), 1.99 (s, 3 H, Me, Ac-4), 2.00 (s, 3 H, Me, Ac-3), 2.02 (s, 3 H, Me, Ac-2), 3.52 (dt, $J_{5,4}$ = 9.7, $J_{5,6}$ = 3.8 Hz, 1 H, H^5), 3.66 (d, $J_{6,5}$ = 3.8 Hz, 2 H, H^6), 4.71 (d, $J_{1,2}$ = 7.7 Hz, 1 H, H^1), 4.90 (dd, $J_{2,3}$ = 9.7, $J_{2,1}$ = 7.7 Hz, 1 H, H^2), 5.02 (t, $J_{4,3}$ = $J_{4,5}$ = 9.7 Hz, 1 H, H^4), 5.16 (t, $J_{3,2}$ = $J_{3,4}$ = 9.7 Hz, 1 H, H^3) ppm. ^{13}C NMR (150 MHz, $CDCl_3$, 25 °C): δ = –5.6, –5.5, –5.4, –4.3 [(CH_3)$_2$Si], 17.8, 18.3 [(CH_3)$_3$*C*], 20.7 (CH_3, 3 Ac), 25.4, 25.8 [(CH$_3$)$_3$C], 62.4 (C^6), 69.1 (C^4), 73.2 (C^3), 73.4 (C^2), 74.8 (C^5), 95.6 (C^1), 169.2 (CO, Ac-2), 169.3 (CO, Ac-3), 170.5 (CO, Ac-4) ppm.

Supporting Information (see also the footnote on the first page of this article): CICSs and nonequivalences of methine proton of **8** (5 mM) in the presence of equimolar amounts of CSA **1**. Diffusion coefficients of TMS and CSA **1** at different concentrations. Determination of heteroassociation constants (Foster–Fyfe method) for (*S*)-**8/1** and (*R*)-**8/1** and for (*S*)-**8/5b** and (*S*)-**8/6b**. Graphical representation of two adjacent glucopyranose rings of a cyclodextrin.

Acknowledgments

The work was supported by the Ministero dell'Università e della Ricerca (MIUR) (Project "High performance separation systems based on chemo- and stereoselective molecular recognition" grant 2005037725, and Fondo per gli Investimenti della Ricerca di Base (FIRB) Project RBPR05NWWC).

[1] J. Snopek, E. Smolkova-Keulemansova, T. Czerh'ati, K. H. Gahm, A. Stalcup, in *Comprehensive Supramolecular Chemistry*, vol. 3, Cyclodextrins (Eds.: J. Szejtli, T. Osa), chapter 18: *Cyclodextrins in Analytical Separation Methods*, Pergamon, **1996**, pp. 515–571.
[2] W. A. König, *Enantioselective Gas Chromatography with Modified Cyclodextrins*, Hüthig, Heidelberg, **1992**.
[3] D. Wistuba, J. Kang, V. Schurig, *Methods Mol. Biol.* **2004**, *243*, 401–409.
[4] C. R. Mitchell, D. W. Armstrong, *Methods Mol. Biol.* **2004**, *243*, 61–112.
[5] U. Schmitt, S. K. Branch, U. Holzgrabe, *J. Sep. Sci.* **2002**, *25*, 959–974.
[6] V. Schurig, *TrAC Trends Anal. Chem.* **2002**, *21*, 647–661.
[7] Z. Juvancz, J. Szejtli, *TrAC Trends Anal. Chem.* **2002**, *21*, 379–388.
[8] A. F. Casy, *TrAC Trends Anal. Chem.* **1993**, *12*, 185–189.
[9] V. Schurig, *Methods of Organic Chemistry (Houben-Weyl), Stereoselective Synthesis*, vol. E21a, Thieme, Stuttgart, New York, *Determination of Enantiomeric Purity by Direct Methods*, chapter 3.1.4: *NMR-Spectroscopy*, **1995**, 157–168.
[10] R. Rothchild, *Enantiomer* **2000**, *5*, 457–471.
[11] T. J. Wenzel, J. D. Wilcox, *Chirality* **2003**, *15*, 256–270.
[12] H. Dodziuk, V. Kozminski, A. Ejchart, *Chirality* **2004**, *16*, 90–105.
[13] B. Chankvetadze, *Chem. Soc. Rev.* **2004**, *33*, 337–347.
[14] G. Uccello-Barretta, F. Balzano, P. Salvadori, *Curr. Pharm. Des.* **2006**, *12*, 4023–4045.
[15] D. Greatbanks, R. Pickford, *Magn. Reson. Chem.* **1987**, *25*, 208–215.
[16] A. F. Casy, A. D. Mercer, *Magn. Reson. Chem.* **1988**, *26*, 765–774.
[17] J. L. Atwood, J. E. D. Davies, D. D. Macnicol, F. Vögtle, *Comprehensive Supramolecular Chemistry*, vol. 3, Cyclodextrins (Eds.: J. Szejtli, T. Osa), Pergamon Press, UK, **1996**.
[18] G. Uccello-Barretta, F. Balzano, A. M. Caporusso, A. Iodice, P. Salvadori, *J. Org. Chem.* **1995**, *60*, 2227–2231.
[19] H.-J. Schneider, F. Hacket, V. Rüdiger, H. Ikeda, *Chem. Rev.* **1998**, *98*, 1755–1785.
[20] G. Uccello-Barretta, F. Balzano, G. Sicoli, A. Scarselli, P. Salvadori, *Eur. J. Org. Chem.* **2005**, 5349–5355.
[21] G. Uccello-Barretta, G. Sicoli, F. Balzano, V. Schurig, P. Salvadori, *Tetrahedron: Asymmetry* **2006**, *17*, 2504–2510.
[22] G. Uccello-Barretta, S. Nazzi, F. Balzano, P. A. Levkin, V. Schurig, P. Salvadori, *Eur. J. Org. Chem.* **2007**, 3219–3226.
[23] A. Dietrich, B. Maas, V. Karl, P. Kreis, D. Lehmann, B. Weber, A. Mosandl, *J. High Resolut. Chromatogr., Chromatogr. Commun.* **1992**, *15*, 176–179.
[24] G. Sicoli, Z. Jiang, L. Jicsinszky, V. Schurig, *Angew. Chem. Int. Ed.* **2005**, *44*, 4092–4095.
[25] G. Sicoli, F. Pertici, Z. Jiang, L. Jicsinszky, V. Schurig, *Chirality* **2007**, *19*, 391–400.
[26] C. S. Johnson Jr, *Prog. Nucl. Magn. Reson. Spectrosc.* **1999**, *34*, 203–256.
[27] *Magn. Reson. Chem.* **2002**, 40 [Special Issue (NMR and Diffusion)], S1–S152.
[28] T. Brand, E. J. Cabrita, S. Berger, *Prog. Nucl. Magn. Reson. Spectrosc.* **2005**, *46*, 159–196.
[29] L. Fielding, *Tetrahedron* **2000**, *56*, 6151–6170.
[30] R. Wimmer, F. L. Aachmann, K. L. Larsen, S. B. Petersen, *Carbohydr. Res.* **2002**, *337*, 841–849.
[31] D. Zuccaccia, A. Macchioni, *Organometallics* **2005**, *24*, 3476–3486.
[32] H. C. Chen, S. H. Chen, *J. Phys. Chem.* **1984**, *88*, 5118–5121.
[33] E. Yumet, H. C. Chen, S. H. Chen, *AIChE J.* **1985**, *31*, 76–81.
[34] A. Gierer, K. Wirtz, *Z. Naturforsch., Teil A* **1953**, *8*, 532–538.
[35] A. Spernol, K. Wirtz, *Z. Naturforsch., Teil A* **1953**, *8*, 522–532.
[36] E. J. Cabrita, S. Berger, *Magn. Reson. Chem.* **2001**, *39*, S142–S148.
[37] R. Foster, C. A. Fyfe, *Trans. Faraday Soc.* **1965**, *61*, 1626–1631.
[38] R. Foster, C. A. Fyfe, *Chem. Commun. (London)* **1965**, 642–643.
[39] K. Takeo, H. Mitoh, K. Uemura, *Carbohydr. Res.* **1989**, *187*, 203–221.
[40] A. R. Khan, P. Forgo, K. J. Stine, V. T. D'Souza, *Chem. Rev.* **1998**, *98*, 1977–1996.
[41] G. Uccello-Barretta, G. Sicoli, F. Balzano, P. Salvadori, *Carbohydr. Res.* **2005**, *340*, 271–281.
[42] J. J. Chambers, D. M. Kurrasch-Orbaugh, M. A. Parker, D. E. Nichols, *J. Med. Chem.* **2001**, *44*, 1003–1010.
[43] P. A. Levkin, A. Ruderisch, V. Schurig, *Chirality* **2006**, *18*, 49–63.

Received: November 26, 2007
Published Online: February 26, 2008

